Editors' Suggestion

Floquet Spin Amplification

Min Jiang,[1,2] Yushu Qin,[1,2] Xin Wang,[1,2] Yuanhong Wang,[1,2] Haowen Su,[1,2] Xinhua Peng,[1,2,*] and Dmitry Budker[3,4,5]

[1]*CAS Key Laboratory of Microscale Magnetic Resonance and School of Physical Sciences, University of Science and Technology of China, Hefei, Anhui 230026, China*
[2]*CAS Center for Excellence in Quantum Information and Quantum Physics, University of Science and Technology of China, Hefei, Anhui 230026, China*
[3]*Helmholtz-Institut, GSI Helmholtzzentrum für Schwerionenforschung, Mainz 55128, Germany*
[4]*Johannes Gutenberg University, Mainz 55128, Germany*
[5]*Department of Physics, University of California, Berkeley, California 94720-7300, USA*

(Received 22 December 2021; revised 18 April 2022; accepted 19 May 2022; published 9 June 2022)

Detection of weak electromagnetic waves and hypothetical particles aided by quantum amplification is important for fundamental physics and applications. However, demonstrations of quantum amplification are still limited; in particular, the physics of quantum amplification is not fully explored in periodically driven (Floquet) systems, which are generally defined by time-periodic Hamiltonians and enable observation of many exotic quantum phenomena such as time crystals. Here we investigate the magnetic-field signal amplification by periodically driven ^{129}Xe spins and observe signal amplification at frequencies of transitions between Floquet spin states. This "Floquet amplification" allows us to simultaneously enhance and measure multiple magnetic fields with at least one order of magnitude improvement, offering the capability of femtotesla-level measurements. Our findings extend the physics of quantum amplification to Floquet spin systems and can be generalized to a wide variety of existing amplifiers, enabling a previously unexplored class of "Floquet spin amplifiers".

DOI: 10.1103/PhysRevLett.128.233201

Quantum amplification that offers the capability of enhancing weak signals is ubiquitous and of central importance to various frontiers of science, ranging from low-noise masers [1–4], ultrasensitive magnetic resonance spectroscopy [5], weak field and force measurements [6–8], and optical amplifiers [9], to hypothetical-particle searches beyond the standard model [10–13]. To date, the well-established paradigm for realizing signal amplification mostly relies on using inherent discrete transitions of quantum systems [14], including atomic and molecular ensembles [5,12,13,15], superconducting qubits, color centers in diamond [1–3], trapped-ion qubits [6,16], etc. However, realizations of quantum amplification are still limited in practice due to restricted tunability and lack of experimentally accessible frequencies of inherent discrete transitions, limiting the performance of quantum amplifiers, for example, in operation bandwidth, frequency, and gain.

Recent years have witnessed increasing attention to periodically driven (Floquet) systems [17,18], which can be described by a series of Floquet states and energies that are analogous to the Brillouin-zone artificial dimension [19]. Floquet systems could be a promising platform to explore advanced quantum amplification beyond ordinary systems, partially because such systems provide an ideal way to engineer the inherent discrete states and transitions of quantum systems. This enables a variety of novel functionalities that might not be otherwise directly accessible, for example, time crystals [20], a Floquet maser [15,21], Floquet Raman transition [22], prethermalization [23], Floquet cavity electromagnonics [24], Floquet polaritons [25], and a Floquet quantum detector [26]. The potential combination of quantum amplification and Floquet systems may open opportunities for developing new quantum amplifiers with improved performance, for example, in operation bandwidth, frequency tunability, and evading the need for population inversion. Such amplifiers would find promising applications in, for example, a topologically protected traveling wave parametric amplifier [27], simultaneous sensing of multiple magnetic fields at different frequencies [28], measurement of the worldwide magnetic-background noise (including Schumann resonance) [29], and searches for axionlike dark matter with multiple sensitive windows of particle mass [10–12].

In this Letter, we report the theoretical and experimental demonstration of quantum amplification on periodically driven spins. The key ingredient is the use of an ensemble of long-lived hyperpolarized ^{129}Xe spins as a periodically driven system, which overlaps with optically polarized ^{87}Rb atoms in the same vapor cell, with Fermi-contact collisions between them. Unlike conventional quantum amplification that exploits inherent transitions [1–8,10–13], we demonstrate that the driven ^{129}Xe spins as an amplifier can

simultaneously amplify external magnetic fields that oscillate at frequencies of transitions between Floquet states, by a factor of more than 10. In addition, we show that the application of certain periodic driving enables spin-amplification gain below one, providing an ideal way to suppress environmental magnetic noise disturbance. The present amplification phenomena on Floquet systems are collectively named "Floquet amplification." In contrast to the well-known amplification by stimulated emission of radiation (maser) that requires population inversion [1–3,5], Floquet amplification removes the population-inversion requirement and highlights the practical applications of building a new class of quantum amplifiers that could operate in ambient conditions. As a first application, our amplifier constitutes a new technology for measuring magnetic fields with broad bandwidth and $\mathrm{fT}/\mathrm{Hz}^{1/2}$-level sensitivity, which is notably better than that of other state-of-the-art magnetometers demonstrated with nuclear spins limited to a sensitivity of a few $\mathrm{pT}/\mathrm{Hz}^{1/2}$. The present amplification technique also allows one to search for hypothetical particles with a sensitivity well beyond the most stringent existing constraints [12,30].

We employ a two-level spin system as a test bed of Floquet amplification. A bias magnetic field B_0 is applied along $\hat{z}$, where the spin Larmor frequency is $\nu_0 = \gamma_n B_0$ and γ_n denotes the gyromagnetic ratio. To periodically drive the spins into a Floquet system, we introduce an oscillating (ac) field $B_{\mathrm{ac}} \cos(2\pi\nu_{\mathrm{ac}} t)\hat{z}$. As a result, the spin Hamiltonian $H(t)$ becomes time periodic but can be mapped into a time-independent Floquet Hamiltonian with infinite dimension [15,19]. As shown in Fig. 1(a), the original two-level system now is expanded to infinite Floquet levels with equal interval ν_{ac}, i.e., $|\uparrow\rangle$ turns into $|\uparrow\rangle_n$, and $|\downarrow\rangle$ turning into $|\downarrow\rangle_m$ [31], where n and m represent the photon number of the periodic driving field and are non-negative integers. With synthetic dimensions supported by Floquet states, the number of resonance transitions increases, thus improving the operation bandwidth and enabling us to constitute multimode amplifiers.

We perform Floquet-amplification experiments with ^{129}Xe noble gas. The setup is described in the Supplemental Material [31] in detail and is similar to that of Refs. [12,13]. As shown in Fig. 1(b), 5-torr ^{129}Xe gas overlaps with enriched ^{87}Rb in a 0.5-cm^3 cubic vapor cell. The vapor cell is enclosed in a boron nitride ceramics and heated to ~160 °C with twisted-pair copper wires. Circularly polarized laser light tuned to the D1 line at 795 nm polarizes ^{87}Rb atoms, and ^{129}Xe spins are polarized through spin-exchange collisions with polarized ^{87}Rb atoms. The spin polarization of ^{129}Xe gas is estimated to be about 30%. We introduce an ac field B_{ac} along $\hat{z}$ for periodic driving of ^{129}Xe. When a transverse oscillating magnetic field matches one of the Floquet ^{129}Xe transitions [for example, $|\downarrow\rangle_m \rightarrow |\uparrow\rangle_n$ in Fig. 1(a)], the polarized ^{129}Xe spins are tilted away from the $\hat{z}$ direction and

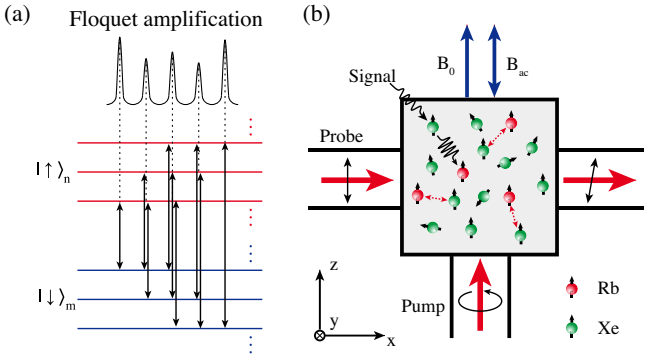

FIG. 1. (a) A periodically driven two-level system can be described by a series of Floquet states $|\uparrow\rangle_n$, $|\downarrow\rangle_m$. We study the transitions between these Floquet states. (b) Schematic of experimental setup. The key element is a cubic vapor cell containing 5 torr ^{129}Xe, 250 torr N_2, and a droplet of isotopically enriched ^{87}Rb. ^{87}Rb atoms are polarized by a circularly polarized laser at 795 nm and probed by a linearly polarized light blue-detuned 110 GHz from the D2 transition at 780 nm. ^{129}Xe spins are polarized by spin-exchange collisions with polarized ^{87}Rb atoms. An oscillating magnetic field as a periodic driving on ^{129}Xe is applied along $\hat{z}$. The driven ^{129}Xe can amplify the magnetic field that oscillates at frequencies of transitions between Floquet states [see (a)]. The amplified field then is *in situ* read out by the ^{87}Rb magnetometer.

accordingly generate oscillating transverse magnetization $\mathbf{M}_n(t)$. The Fermi-contact collisions between ^{129}Xe and ^{87}Rb lead to that ^{87}Rb experiences an effective magnetic field [38–40], $\mathbf{B}_{\mathrm{eff}} = (8\pi\kappa_0/3)\mathbf{M}_n(t)$, which is *in situ* read out by ^{87}Rb magnetometer [41–43]. Here $\kappa_0 \approx 540$ denotes the Fermi-contact enhancement factor between ^{129}Xe and ^{87}Rb [44]. As a result, the magnetic field $\mathbf{B}_{\mathrm{eff}}$ generated by ^{129}Xe nuclear magnetization can be enhanced by a large factor of κ_0, and can be significantly larger than the measured field.

Using synthetic dimensions supported by Floquet states, the magnetic field can be amplified at a series of comblike frequencies $\nu_0, \nu_0 \pm \nu_{\mathrm{ac}}, \ldots, \nu_0 \pm k\nu_{\mathrm{ac}}, \cdots$, which correspond to k-photon transitions (or sidebands). We define the amplification factor as the ratio between the effective field $\mathbf{B}_{\mathrm{eff}}$ and the measured field $\mathbf{B}_s$, i.e., $|\mathbf{B}_{\mathrm{eff}}/\mathbf{B}_s|$. We show that the k-photon amplification to the signal is [31]

$$\eta_{k,0}(u) = \frac{4\pi}{3}\kappa_0 M^n P_0^n \gamma_n T_{2n} J_k^2(u), \tag{1}$$

where P_0^n is the equilibrium polarization of ^{129}Xe, M^n is the magnetization ^{129}Xe atoms with unity polarization, $\gamma_n \approx 0.01178$ Hz/nT is the gyromagnetic ratio of ^{129}Xe, $T_{2n} \approx 34$ s is the transverse relaxation time of ^{129}Xe spins, J_k is the Bessel function of the first kind of order k, and $u = \gamma_n B_{\mathrm{ac}}/\nu_{\mathrm{ac}}$ is the modulation index.

Figure 2(a) shows the experimental data on Floquet amplification. The parameters are set as $B_0 \approx 853$ nT,

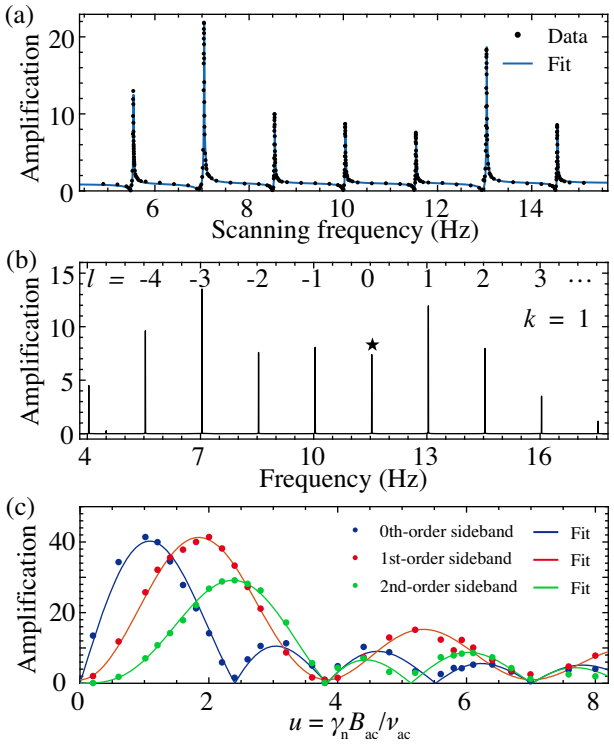

FIG. 2. (a) Plot of amplification as a function of the scanning test-field frequency. The bias field and periodic driving field are set as $B_0 \approx 853$ nT, $B_{\rm ac} \approx 397$ nT, $\nu_{\rm ac} \approx 1.500$ Hz. The corresponding modulation index is $u \approx 3.12$. The interval between amplification frequencies is 1.500 Hz that is equal to $\nu_{\rm ac}$. The amplification at each resonance frequency satisfies $\eta_{k,0}$ [see Eq. (1)]. The amplification profile is asymmetric due to the Fano interference described in the text. (b) Spectrum of the amplification signal induced by a test field. The test signal is set at the frequency of the first-order sideband (see star) and there simultaneously exist other sideband signals. The amplification satisfies $\eta_{k,l}$ [see Eq. (2)]. (c) Plot of Floquet amplification as a function of the modulation index u. A periodic driving field of $\nu_{\rm ac} \approx 3.000$ Hz is introduced. By scanning the amplitude $B_{\rm ac}$, the amplification of the test signal at 7.039 Hz (red points) follows $J_1^2(u)$ (red line). The amplification at 10.039 Hz (blue points) follows $J_1(u)J_0(u)$ (blue line) and at 4.039 Hz (green points) follows $J_1(u)J_2(u)$ (green line).

$B_{\rm ac} \approx 397$ nT, $\nu_{\rm ac} \approx 1.500$ Hz, corresponding to $\nu_0 \approx 10.039$ Hz and modulation index $u \approx 3.12$. A transverse oscillating magnetic field as a test signal is applied along $\hat{y}$, and its frequency is scanned from about 4.900 Hz to 15.100 Hz. Considering that the resonance linewidth is as narrow as ≈17 mHz determined by $\sqrt{3}/(\pi T_{2n})$ [31], the scanning frequency step is set as 1 mHz around resonance frequencies. To determine the amplification factor, we record the ^{87}Rb magnetometer response signal far way from resonance as a reference. All signal strengths are obtained by performing Fourier transform of the magnetometer signals. The experimental result is shown in Fig. 2(a) and the ratio among different transitions is close to the theoretical value $J_0^2(u):J_{\pm1}^2(u):J_{\pm2}^2(u):J_{\pm3}^2(u) = 1:0.969:2.660:1.225$.

An amplification phenomenon is observed on Floquet ^{129}Xe spins. Specifically, although the test frequency matches only one Floquet transition, there simultaneously exist amplification signals at other Floquet transitions. For example shown in Fig. 2(b), there is a peak at the frequency of the test field set at 11.539 Hz (marked with a star), and otherwise there exist other sidebands even with larger signal amplitude. These sidebands are similar to frequency comb composed of equidistant narrow lines, and can be seen as the result of the test-field photons scattered by driven ^{129}Xe spins, where the virtual absorption and emission of ac photons occur [31]. We obtain the corresponding amplification factor [31]

$$\eta_{k,l}(u) = \frac{4}{3}\kappa_0 M^n P_0^n \gamma_n T_{2n} J_{l+k}(u) J_k(u), \tag{2}$$

where k is the order of the sideband where the test field is located, l is the order difference between the test-field sideband and other induced sideband [see an example in Fig. 2(b)]. Obviously, the amplification factor $\eta_{k,l}(u)$ becomes the same with that described in Eq. (1) when $l = 0$. In the experiment of Fig. 2(b), $k = 1$ (matching the first-order sideband). We obtain the experimental ratio between different cross-amplification lines, i.e., $\eta_{1,-1}:\eta_{1,0}:\eta_{1,1}:\eta_{1,2} \approx 1:0.916:1.480:0.987$, which is in agreement with the theoretical value: $|J_0(u)|:|J_1(u)|:|J_2(u)|:|J_3(u)| = 1:0.984:1.631:1.107$.

We find an analytical relation for power amplification:

$$\sum_{l=-\infty}^{+\infty} \eta_{k,l}^2(u) = \eta_{0,0}(0)\eta_{k,0}(u), \tag{3}$$

indicating the total power at all Floquet transitions remaining a constant for a measurement. This kind of Floquet amplification is well suited for eliminating uncorrelated noise. For example, we employ frequency-comb-like seven sidebands shown in Fig. 2(b) as detection indicators. A true event should induce detectable signals at all sidebands. In contrast to the detection with a single sideband where the noise-induced false alarm rate is 5% (95% confidence level), the simultaneous detection with seven sidebands would reduce the false-positive rate down to 7.8×10^{-10}, with 7 orders of magnitude improvement. This would provide a high-confidence-level way to identify an event from random noise. In this work, we only consider an event with classical magnetic field that induces detectable signals at all sidebands. However, we should note that it is only possible to detect a single sideband when the measured field is as low as the single-photon level.

The amplification $\eta_{k,l}(u)$ is adjustable by changing modulation index u according to Eq. (2). We set the resonance frequency of ^{129}Xe at $\nu_0 \approx 10.039$ Hz and the

periodic driving frequency at $\nu_{ac} \approx 3.000$ Hz. The index u is scanned from 0 to 8.00 by changing driving amplitudes. The test-field frequency is applied, for example, at the first-order sideband $\nu_0 - \nu_{ac} \approx 7.039$ Hz. In this case, we plot the amplification factors of three sidebands as a function of u, as shown in Fig. 2(c). The zeroth at ν_0, first sideband at $\nu_0 - \nu_{ac}$, and second-sideband at $\nu_0 - 2\nu_{ac}$ well follow theoretical profiles $J_1(u)J_0(u)$ (blue line), $J_1^2(u)$ (red line), and $J_1(u)J_2(u)$ (green line), respectively. The modulation index u can be optimized to maximize the amplification. For example, when u is close to the theoretical value 1.84, the first-order amplification (red line) reaches the maximum 41.4 (i.e., 32.3 dB).

We demonstrate the magnetic-field sensitivity of our technique based on Floquet spin amplification. Figure 3 shows the case of a 1.5-Hz periodic driving and modulation index $u \approx 1.4$. In this case, the achieved magnetic sensitivity is about 20 $\mathrm{fT/Hz^{1/2}}$, 25 $\mathrm{fT/Hz^{1/2}}$, 18 $\mathrm{fT/Hz^{1/2}}$ at $\nu_0 - 1.5$, ν_0, $\nu_0 + 1.5$, respectively. Our result illustrates that the magnetic sensitivity can be simultaneously enhanced to $\mathrm{fT/Hz^{1/2}}$ level at frequencies of transitions between Floquet spin states. Moreover, the sensitivity at different Floquet-transition frequencies can be controlled through changing modulation index. In the Supplemental Material [31], we demonstrate the direct measurements of femtotesla-level magnetic fields using the Floquet-spin-amplification technique and further discuss the typical noise that limit our current sensitivity.

The line shape of amplification as a function of scanning frequency is not symmetric under a certain regime, as shown in Fig. 2(a). We find that the asymmetric line originates from the well-known Fano resonance [45–47]. Specifically, the ^{87}Rb and ^{129}Xe spins simultaneously experience the applied test field and both independently generate signals at the test frequency. To appear the Fano resonance, a discrete-level system and a continuum-level system should exist. In our case, ^{129}Xe spins have a sharp resonance line and thus can be seen as a discrete system, whereas ^{87}Rb spins have a broad resonance line and can be approximated as a continuum system. The phase of ^{129}Xe induced signal changes rapidly near resonance, while the phase of ^{87}Rb signal varies slowly. Because of the phase difference between their signals, the ^{129}Xe induced and direct ^{87}Rb signals interfere with each other and their interference gives rise to the asymmetric line shape, where a destructive interference occurs on the left and a constructive interference occurs on the right side of the resonance [see Fig. 2(a)]. Notably, due to the destructive interference, the amplification factor could be smaller than one when the scanning test frequency is nearby Floquet transitions. A detailed theoretical model of Fano resonance is presented in the Supplemental Material [31].

Because of the existence of a Fano resonance as described above, the amplifier reduces the response to the test field and can be adjusted to be insensitive to environmental magnetic noise. We quantify the response reduction under a different modulation index u. We set $\nu_0 \approx 10.039$ Hz and $\nu_{ac} \approx 13.000$ Hz. The first-order sideband frequency is at 2.971 Hz. When the modulation index u is scanned from 3.44 to 3.66 by changing B_{ac}, the amplification factor is smaller than one, turning into a deamplification regime. For example, the amplification reduces down to $\eta_1 \approx 0.2$ when $u \approx 3.50$, indicating that the response of magnetic field noise can be suppressed by a factor of about 5. As shown in the inset of Fig. 4, when the

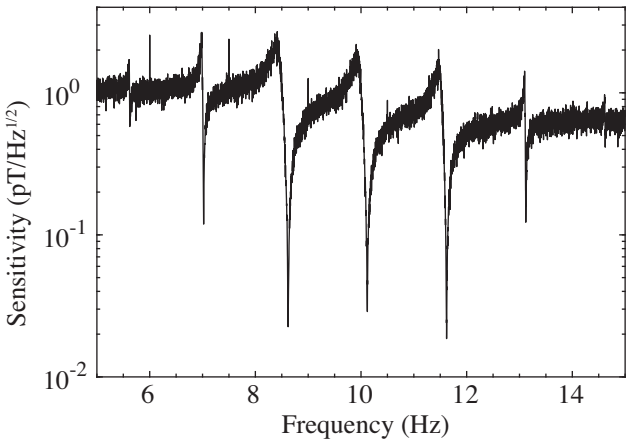

FIG. 3. The magnetic sensitivity of the Floquet-amplification-based magnetometer. The bias field and periodic driving field are set as $B_0 \approx 853$ nT, $B_{ac} \approx 178$ nT, and $\nu_{ac} \approx 1.500$ Hz. The corresponding modulation index is $u \approx 1.4$. The sensitivity is about 20 $\mathrm{fT/Hz^{1/2}}$, 25 $\mathrm{fT/Hz^{1/2}}$, 18 $\mathrm{fT/Hz^{1/2}}$ at $\nu_0 - 1.5$, ν_0, $\nu_0 + 1.5$, respectively. The line shape is asymmetric due to the Fano resonance.

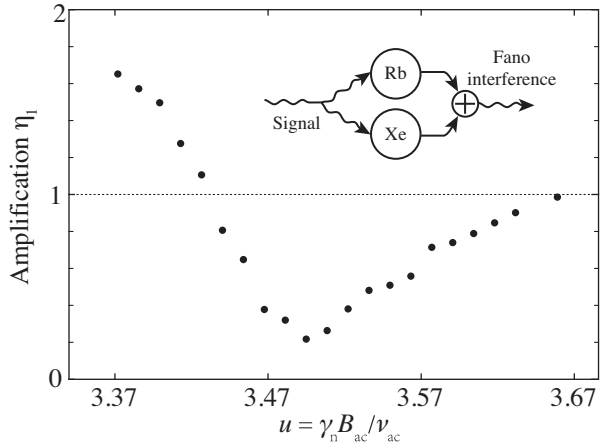

FIG. 4. Fano resonance in spin amplification. Black points denote the measured amplification of the test-field signal at 2.970 Hz with the parameters of $\nu_0 \approx 10.039$ Hz and $\nu_{ac} \approx 13.000$ Hz. The signal amplitude is suppressed by a factor of 5 when the modulation index is $u \approx 3.497$. In the inset, the ^{129}Xe-^{87}Rb signals interfere with each other and their interference results in suppressing amplification.

effective field of ^{129}Xe and test signal have different phase, destructive interference occurs and noise suppression appears. A similar mechanism of noise suppression has been reported in a self-compensating comagnetometer [40,48]. However, comagnetometers usually work for suppressing adiabatically changing (low-frequency) magnetic noise, our amplifier provides the capability of suppressing high-frequency magnetic noise. Although insensitive to actual magnetic field in certain regimes, our amplifier remains sensitive to some beyond-the-standard-model exotic fields that couple with only one of the ^{129}Xe and ^{87}Rb [10,12,13,49].

The present Floquet amplification can be used for a broad range of applications in precision measurements. For example, the application of Floquet amplification to magnetic field sensing, which is capable of simultaneously measuring fields at Floquet transitions, yields one order of magnitude improvements over previously achievable detection bandwidth [12,13]. Based on the demonstrations in this work, the magnetic field sensitivity is in the range of tens $\mathrm{fT}/\mathrm{Hz}^{1/2}$, and can be further improved to $\mathrm{aT}/\mathrm{Hz}^{1/2}$ level using the K-^{3}He system due to the longer ^{3}He coherence time [12,13].

Our amplifier can be also applied to search for hypothetical particles predicted by numerous theories beyond the standard model [50,51], such as ultralight axions and dark photons. These particles are predicted to couple with standard model particles (such as nuclear spins) and behave as an oscillating magnetic field [11,52], which can be greatly amplified with our amplifier. As a result, it is promising to improve the search sensitivity of axions and dark photons with new limits beyond the astrophysical ones. Importantly, to complete the searches for a full range of particle masses, the traditional approaches have to perform measurements and scan with a single bandwidth [10–12,52–54], which is time consuming and limits experimental searches. In contrast, our approach can simultaneously measure the exotic fields with multiple detection bandwidths. We perform an experimental test and show that the present Floquet-amplification technique speeds up the total measurement time by a factor of about 3 (see Supplemental Material [31] for details). Moreover, the Floquet amplification provides an ideal way to distinguish the exotic-field signal from spurious random noise with a false-positive rate as low as $\sim 10^{-9}$.

In conclusion, we have reported a demonstration of spin amplification on periodically driven (Floquet) ^{129}Xe spins. The successful combination of quantum amplification and Floquet systems allows for observing a class of Floquet amplification phenomena, which are not accessible in previous studies. Our findings improve the detection bandwidth by one order of magnitude and make it possible to build a new type of quantum amplifiers that allow simultaneously amplifying the electromagnetic wave at multiple frequencies. Such properties of amplifiers will be essential for low-energy searches for hypothetical particles beyond the standard model [12,13]. Although demonstrated for the ^{129}Xe system, our scheme of Floquet amplification is generic and can be applied to a wide range of quantum amplifiers. For example, recent advances in pentacene molecules [3,55] and nitrogen-vacancy defect materials [1,2] have led to progress in areas of low-noise room-temperature amplifiers. The combination of such amplifiers and periodic driving (for example, with the use of an oscillating magnetic field) could increase the detection regimes that could find attractive applications in cosmological observation and deep-space communications.

We thank Dong Sheng, Hao Wu, Jianmin Cai, Renbao Liu, and Itay Bloch for valuable discussions. This work was supported by National Key Research and Development Program of China (Grant No. 2018YFA0306600), National Natural Science Foundation of China (Grants No. 11661161018, No. 11927811, No. 12004371), Anhui Initiative in Quantum Information Technologies (Grant No. AHY050000), and USTC Research Funds of the Double First-Class Initiative (Grant No. YD3540002002). This work was also supported in part by the Cluster of Excellence "Precision Physics, Fundamental Interactions, and Structure of Matter" (PRISMA+ EXC 2118/1) funded by the German Research Foundation (DFG) within the German Excellence Strategy (Project ID 39083149).

M. J., Y. Q., and X. W. contributed equally to this work.

*xhpeng@ustc.edu.cn

[1] J. D. Breeze, E. Salvadori, J. Sathian, N. M. Alford, and C. W. Kay, Continuous-wave room-temperature diamond maser, Nature (London) **555**, 493 (2018).
[2] L. Jin *et al.*, Proposal for a room-temperature diamond maser, Nat. Commun. **6**, 1 (2015).
[3] M. Oxborrow, J. D. Breeze, and N. M. Alford, Room-temperature solid-state maser, Nature (London) **488**, 353 (2012).
[4] K. Chu, The electron cyclotron maser, Rev. Mod. Phys. **76**, 489 (2004).
[5] M. Suefke, S. Lehmkuhl, A. Liebisch, B. Blümich, and S. Appelt, Para-hydrogen raser delivers sub-millihertz resolution in nuclear magnetic resonance, Nat. Phys. **13**, 568 (2017).
[6] S. Kotler, N. Akerman, Y. Glickman, A. Keselman, and R. Ozeri, Single-ion quantum lock-in amplifier, Nature (London) **473**, 61 (2011).
[7] S. Burd, R. Srinivas, J. J. Bollinger, A. C. Wilson, D. J. Wineland, D. Leibfried, D. H. Slichter, and D. T. C. Allcock, Quantum amplification of mechanical oscillator motion, Science **364**, 1163 (2019).
[8] J. M. Boss, K. Cujia, J. Zopes, and C. L. Degen, Quantum sensing with arbitrary frequency resolution, Science **356**, 837 (2017).
[9] A. Zavatta, J. Fiurášek, and M. Bellini, A high-fidelity noiseless amplifier for quantum light states, Nat. Photonics **5**, 52 (2011).

[10] R. Bradley, J. Clarke, D. Kinion, L. J. Rosenberg, K. van Bibber, S. Matsuki, M. Mück, and P. Sikivie, Microwave cavity searches for dark-matter axions, Rev. Mod. Phys. **75**, 777 (2003).

[11] D. Budker, P. W. Graham, M. Ledbetter, S. Rajendran, and A. O. Sushkov, Proposal for a Cosmic Axion Spin Precession Experiment (CASPEr), Phys. Rev. X **4**, 021030 (2014).

[12] M. Jiang, H. Su, A. Garcon, X. Peng, and D. Budker, Search for axion-like dark matter with spin-based amplifiers, Nat. Phys. **17**, 14021407 (2021).

[13] H. Su, Y. Wang, M. Jiang, W. Ji, P. Fadeev, D. Hu, X. Peng, and D. Budker, Search for exotic spin-dependent interactions with a spin-based amplifier, Sci. Adv. **7**, eabi9535 (2021).

[14] A. A. Clerk, M. H. Devoret, S. M. Girvin, F. Marquardt, and R. J. Schoelkopf, Introduction to quantum noise, measurement, and amplification, Rev. Mod. Phys. **82**, 1155 (2010).

[15] M. Jiang, H. Su, Z. Wu, X. Peng, and D. Budker, Floquet maser, Sci. Adv. **7**, eabe0719 (2021).

[16] S. Burd, R. Srinivas, H. M. Knaack, W. Ge, A. C. Wilson, D. J. Wineland, D. Leibfried, J. J. Bollinger, D. T. C. Allcock, and D. H. Slichter, Quantum amplification of boson-mediated interactions, Nat. Phys. **17**, 898 (2021).

[17] R. Moessner and S. L. Sondhi, Equilibration and order in quantum floquet matter, Nat. Phys. **13**, 424 (2017).

[18] A. Eckardt, Colloquium: Atomic quantum gases in periodically driven optical lattices, Rev. Mod. Phys. **89**, 011004 (2017).

[19] J. H. Shirley, Solution of the Schrödinger equation with a Hamiltonian periodic in time, Phys. Rev. **138**, B979 (1965).

[20] D. V. Else, B. Bauer, and C. Nayak, Floquet Time Crystals, Phys. Rev. Lett. **117**, 090402 (2016).

[21] R.-B. Liu, A masing ladder, Science **371**, 780 (2021).

[22] Z. Shu, Y. Liu, Q. Cao, P. Yang, S. Zhang, M. B. Plenio, F. Jelezko, and J. Cai, Observation of Floquet Raman Transition in a Driven Solid-State Spin System, Phys. Rev. Lett. **121**, 210501 (2018).

[23] P. Peng, C. Yin, X. Huang, C. Ramanathan, and P. Cappellaro, Floquet prethermalization in dipolar spin chains, Nat. Phys. **17**, 444 (2021).

[24] J. Xu, C. Zhong, X. Han, D. Jin, L. Jiang, and X. Zhang, Floquet Cavity Electromagnonics, Phys. Rev. Lett. **125**, 237201 (2020).

[25] L. W. Clark, N. Jia, N. Schine, C. Baum, A. Georgakopoulos, and J. Simon, Interacting Floquet polaritons, Nature (London) **571**, 532 (2019).

[26] I. M. Bloch, G. Ronen, R. Shaham, O. Katz, T. Volansky, and O. Katz, NASDUCK: New constraints on axion-like dark matter from Floquet quantum detector, Sci. Adv. **8**, eabl8919 (2022).

[27] V. Peano, M. Houde, F. Marquardt, and A. A. Clerk, Topological Quantum Fluctuations and Traveling Wave Amplifiers, Phys. Rev. X **6**, 041026 (2016).

[28] J. Lang, R.-B. Liu, and T. Monteiro, Dynamical-Decoupling-Based Quantum Sensing: Floquet Spectroscopy, Phys. Rev. X **5**, 041016 (2015).

[29] A. Fraser-Smith and J. Buxton, Superconducting magnetometer measurements of geomagnetic activity in the 0.1- to 14-Hz frequency range, J. Geophys. Res. **80**, 3141 (1975).

[30] A. Garcon *et al.*, Constraints on bosonic dark matter from ultralow-field nuclear magnetic resonance, Sci. Adv. **5**, eaax4539 (2019).

[31] See Supplemental Material at http://link.aps.org/supplemental/10.1103/PhysRevLett.128.233201 containing details of experimental apparatus, derivation of Floquet dynamics and Floquet amplification, Fano resonance, and femtotesla-field measurements, which includes Refs. [32–37].

[32] Z. Wu, M. Kitano, W. Happer, M. Hou, and J. Daniels, Optical determination of alkali metal vapor number density using Faraday rotation, Appl. Opt. **25**, 4483 (1986).

[33] W. Opechowski, Magneto-optical effects and paramagnetic resonance, Rev. Mod. Phys. **25**, 264 (1953).

[34] C. Cohen-Tannoudji, G. Grynberg, and J. Dupont-Roc, *Atom-Photon Interactions: Basic Processes and Applications* (Wiley, New York, 1992).

[35] L. Novikov and G. Skrotskiĭ, Nonlinear and parametric effects in atomic rf spectroscopy, Sov. Phys. Usp. **21**, 589 (1978).

[36] D. Budker and F. J. Kimball, *Optical Magnetometry* (Cambridge University Press, Cambridge, Engalnd, 2013), Chap. 12.

[37] T. Kornack, S. Smullin, S.-K. Lee, and M. Romalis, A low-noise ferrite magnetic shield, Appl. Phys. Lett. **90**, 223501 (2007).

[38] M. Bulatowicz, R. Griffith, M. Larsen, J. Mirijanian, C. B. Fu, E. Smith, W. M. Snow, H. Yan, and T. G. Walker, Laboratory Search for a Long-Range T-Odd, P-Odd Interaction from Axionlike Particles Using Dual-Species Nuclear Magnetic Resonance with Polarized ^{129}Xe and ^{131}Xe Gas, Phys. Rev. Lett. **111**, 102001 (2013).

[39] D. Sheng, A. Kabcenell, and M. V. Romalis, New Classes of Systematic Effects in Gas Spin Comagnetometers, Phys. Rev. Lett. **113**, 163002 (2014).

[40] R. Li, W. Fan, L. Jiang, L. Duan, W. Quan, and J. Fang, Rotation sensing using a K-Rb-^{21}Ne comagnetometer, Phys. Rev. A **94**, 032109 (2016).

[41] D. Budker and M. Romalis, Optical magnetometry, Nat. Phys. **3**, 227 (2007).

[42] M. Jiang, W. Xu, Q. Li, Z. Wu, D. Suter, and X. Peng, Interference in atomic magnetometry, Adv. Quantum Technol. **3**, 2000078 (2020).

[43] M. Jiang, R. P. Frutos, T. Wu, J. W. Blanchard, X. Peng, and D. Budker, Magnetic Gradiometer for the Detection of Zero- to Ultralow-Field Nuclear Magnetic Resonance, Phys. Rev. Applied **11**, 024005 (2019).

[44] T. G. Walker and W. Happer, Spin-exchange optical pumping of noble-gas nuclei, Rev. Mod. Phys. **69**, 629 (1997).

[45] U. Fano, Effects of configuration interaction on intensities and phase shifts, Phys. Rev. **124**, 1866 (1961).

[46] B. Luk'yanchuk, N. I. Zheludev, S. A. Maier, N. J. Halas, P. Nordlander, H. Giessen, and C. T. Chong, The Fano resonance in plasmonic nanostructures and metamaterials, Nat. Mater. **9**, 707 (2010).

[47] M. F. Limonov, M. V. Rybin, A. N. Poddubny, and Y. S. Kivshar, Fano resonances in photonics, Nat. Photonics **11**, 543 (2017).

[48] T. Kornack, R. Ghosh, and M. Romalis, Nuclear Spin Gyroscope Based on an Atomic Comagnetometer, Phys. Rev. Lett. **95**, 230801 (2005).

[49] M. Safronova, D. Budker, D. DeMille, D. F. Jackson Kimball, A. Derevianko, and C. W. Clark, Search for new physics with atoms and molecules, Rev. Mod. Phys. **90**, 025008 (2018).

[50] P. W. Graham, D. E. Kaplan, J. Mardon, S. Rajendran, W. A. Terrano, L. Trahms, and T. Wilkason, Spin precession experiments for light axionic dark matter, Phys. Rev. D **97**, 055006 (2018).

[51] P. W. Graham, I. G. Irastorza, S. K. Lamoreaux, A. Lindner, and K. A. van Bibber, Experimental searches for the axion and axion-like particles, Annu. Rev. Nucl. Part. Sci. **65**, 485 (2015).

[52] P. W. Graham and S. Rajendran, New observables for direct detection of axion dark matter, Phys. Rev. D **88**, 035023 (2013).

[53] D. Aybas, J. Adam, E. Blumenthal, A. V. Gramolin, D. Johnson *et al.*, Search for Axionlike Dark Matter Using Solid-State Nuclear Magnetic Resonance, Phys. Rev. Lett. **126**, 141802 (2021).

[54] A. Arvanitaki and A. A. Geraci, Resonantly Detecting Axion-Mediated Forces with Nuclear Magnetic Resonance, Phys. Rev. Lett. **113**, 161801 (2014).

[55] H. Wu, S. Mirkhanov, W. Ng, and M. Oxborrow, Bench-Top Cooling of a Microwave Mode Using an Optically Pumped Spin Refrigerator, Phys. Rev. Lett. **127**, 053604 (2021).